THE JOURNAL OF PHYSICAL CHEMISTRY B

Article

pubs.acs.org/JPCB

# Effects of High Temperature on Desolvation Costs of Salt Bridges Across Protein Binding Interfaces: Similarities and Differences between Implicit and Explicit Solvent Models

Reza Salari and Lillian T. Chong*

Department of Chemistry, University of Pittsburgh, Pittsburgh, Pennsylvania 15260, United States

Supporting Information

**ABSTRACT:** The role of salt bridges in protein−protein binding is largely determined by the costs of desolvating the oppositely charged members of the salt bridge upon binding. On the basis of Poisson−Boltzmann (PB) implicit solvent calculations, it has been proposed that the reduced desolvation penalties of salt bridges at high temperatures provide one explanation for the increased abundance of salt bridges in hyperthermophilic proteins. Here, for the first time, we directly compare the PB implicit solvent model with several explicit water models in computing the effects of extremely high temperature (i.e., 100 °C) on the desolvation penalties of salt bridges across protein−protein interfaces. With the exception of two outliers, the desolvation costs at 100 °C from implicit and explicit solvent calculations are of similar magnitudes and significantly reduced relative to 25 °C. The two outliers correspond to salt bridges that are both buried and part of a salt bridge network, a challenging case that should be considered in the development of fast solvation models.

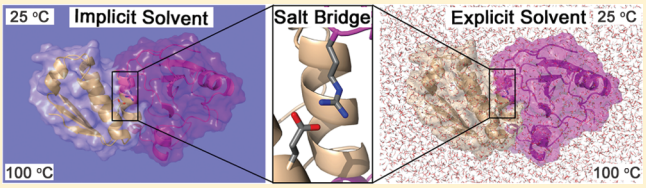


## INTRODUCTION

Salt bridges are thought to make little contribution to the stability of protein−protein complexes at room temperature;[1−3] however, they are particularly abundant in hyperthermophilic proteins[4−7] and therefore appear to play critical roles in the adaptation of proteins for stability at extremely high temperatures (e.g., 100 °C). The latter point has been rationalized on the basis of theoretical studies, which determined the thermodynamic costs of desolvating the oppositely charged members of the salt bridge upon binding to be significant at room temperature[1−3] but markedly reduced at high temperatures.[8] For efficient computations, these studies all employed a dielectric continuum solvent model based on the Poisson−Boltzmann (PB) equation, which is the gold standard of implicit solvent models. Despite the simplicity of the PB model, it has been possible to parametrize the model to reproduce solvation free energies of small organic molecules determined by either experiment[9] or more costly simulations with explicit water molecules.[10,11] In addition, PB calculations have been found to be comparable to explicit solvent simulations in capturing temperature-dependent effects for the association of salt bridge analogues (i.e., acetate and methyl ammonium) from 0 to 100 °C,[12] provided that certain physical parameters are adjusted according to temperature.[13] Nevertheless, the PB model lacks important features such as molecular details of the first solvation shell, including bridging water molecules.[14,15] Valuable insights about modeling solvation effects can therefore be obtained by comparing implicit solvent calculations with more detailed explicit solvent calculations.[12,14−21]

Recently, we conducted a direct comparison of the PB implicit solvent model with several explicit solvent models in computing the desolvation penalties of salt bridges across a number of protein−protein interfaces at 25 °C and found overall agreement between the implicit and explicit solvent results.[14] Here, for the first time, we directly compare implicit and explicit solvent models in computing the desolvation penalties of salt bridges across protein−protein interfaces at high temperature (i.e., 100 °C). Both our comparisons at 25 and 100 °C involve the same set of salt bridges, namely, all 14 salt bridges across the binding interfaces of four protein−protein complexes (Figure 1) that had been identified by others as having a wide range of desolvation penalties.[3] As done in previous theoretical studies on the desolvation penalties of salt bridges,[2,3,14,22−25] we focused on (a) rigid binding, with the unbound conformations of the proteins being identical to the corresponding bound conformations, and (b) evaluating the desolvation penalties relative to those obtained when the charged side-chains are replaced by hydrophobic side-chains of identical size and shape (isosteres), i.e., $\Delta\Delta G_{solv}$; these hydrophobic isosteres are hypothetical mutant versions in which all partial charges on the salt bridge side chains are set to 0. In the implicit solvent calculations, desolvation penalties were computed using the PB model; in the explicit solvent calculations, they were computed using thermodynamic integration techniques (see Methods). We explored the same three explicit water models as our previous study at 25 °C, namely, TIP3P,[26] TIP4P,[26] and SPC/E.[27] Although the dielectric constants of these explicit water models may not be

Received: October 23, 2011
Revised: January 14, 2012
Published: February 2, 2012






dx.doi.org/10.1021/jp210172b | J. Phys. Chem. B 2012, 116, 2561−2567

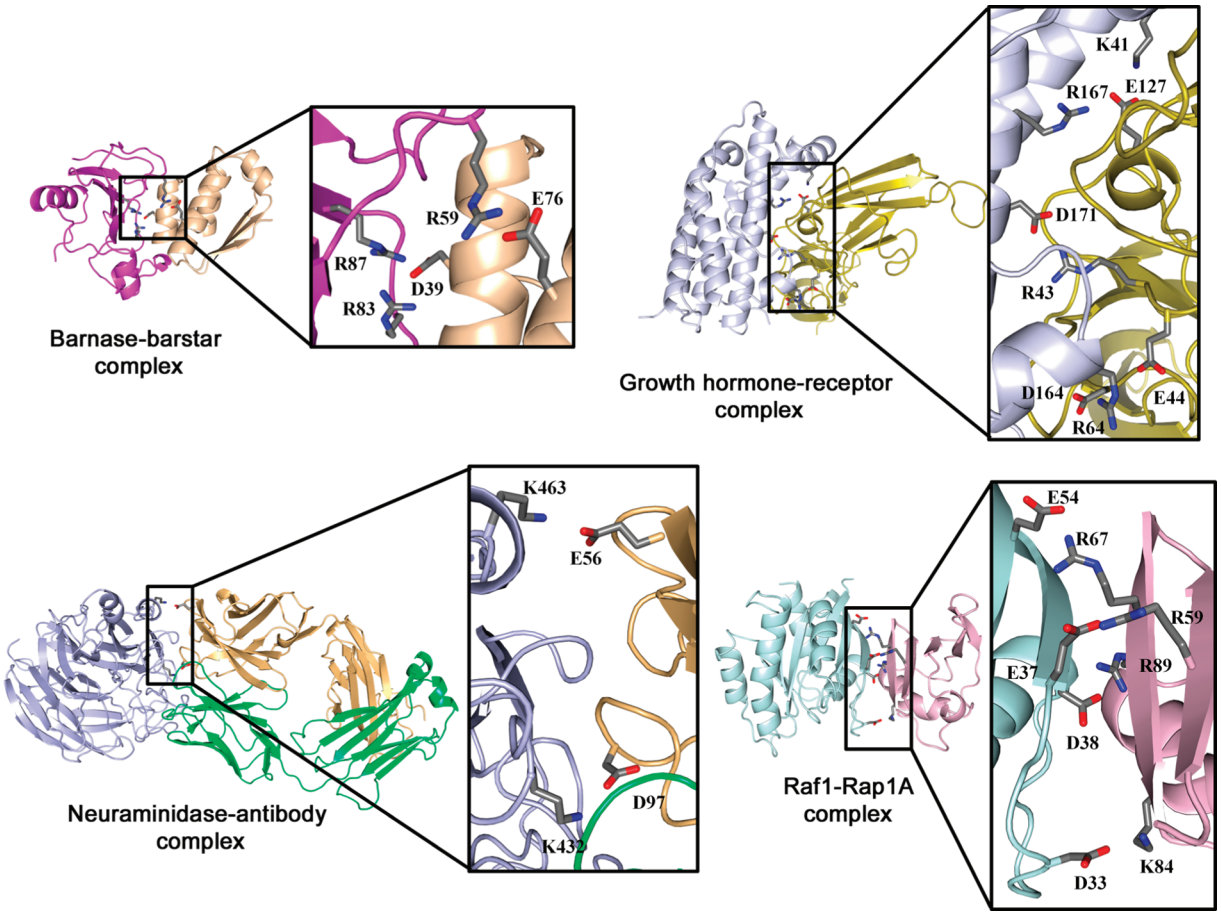


**Figure 1.** Locations of salt bridges across the binding interface of each protein−protein complex in this study.

accurate for a given temperature, their relative changes from one temperature to another are likely to be in good agreement with experiment.[28] We therefore focused our comparison of implicit and explicit solvent models on their computed desolvation penalties of salt bridges at 100 °C *relative to* 25 °C.

## METHODS

In order to directly compare the solvation thermodynamics of the implicit and explicit solvent models, it was essential to keep the proteins completely rigid, even in the explicit solvent molecular dynamics (MD) simulations. It was also necessary to fix all parameters common to the two approaches to ensure that they remained absolutely identical, that is, protein coordinates, atomic charges and radii (OPLS-AA/L force field),[29] box volume, and temperature. Periodic boundary conditions were employed in both approaches, enabling the use of the PME treatment of long-range electrostatics[30] for the explicit solvent calculations. As required by the PME method,[31] all systems were constructed to be electrically neutral by implementing the following in both implicit and explicit solvent calculations: (1) neutralizing the net charge of each protein−protein complex by introducing mutations at the most distant locations from the binding interface,[14] (2) representing the unbound state with the proteins separated by a distance (30 Å between their centers-of-mass) at which electrostatic interactions between the proteins were found to be negligible, and (3) simultaneously mutating the oppositely charged side chains of the salt bridge to their hydrophobic isosteres (i.e., turn off their partial charges) in both the unbound and bound states of the proteins.

Desolvation penalties of salt bridges upon protein binding relative to their hydrophobic isosteres ($\Delta\Delta G_{solv}$) were computed according to the thermodynamic cycle shown in Figure 2. In particular, the $\Delta\Delta G_{solv}$ of each salt bridge was

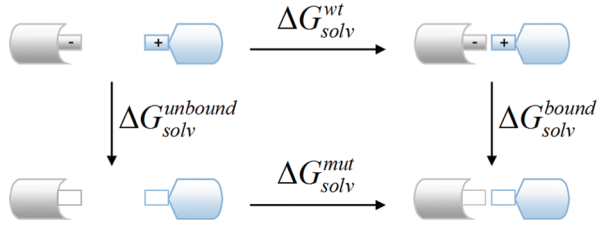


**Figure 2.** Thermodynamic cycle used for computing the desolvation penalty of a salt bridge upon protein binding relative to its hydrophobic isostere ($\Delta\Delta G_{solv}$). The wild-type salt bridge and its mutant hydrophobic isostere are represented by the filled and empty rectangles, respectively.

computed using the following equation, which circumvents the need to simulate the diffusional association of the proteins:

$$\Delta\Delta G_{solv} = \Delta G^{unbound}_{solv} - \Delta G^{bound}_{solv}$$

where $\Delta G^{unbound}_{solv}$ and $\Delta G^{bound}_{solv}$ are the solvation free energies of the wild-type unbound and bound states, respectively, relative to the corresponding mutant hydrophobic isostere states. Full details of the protein models as well as the implicit and explicit solvent calculations are provided in our previous publication


dx.doi.org/10.1021/jp210172b | J. Phys. Chem. B 2012, 116, 2561−2567

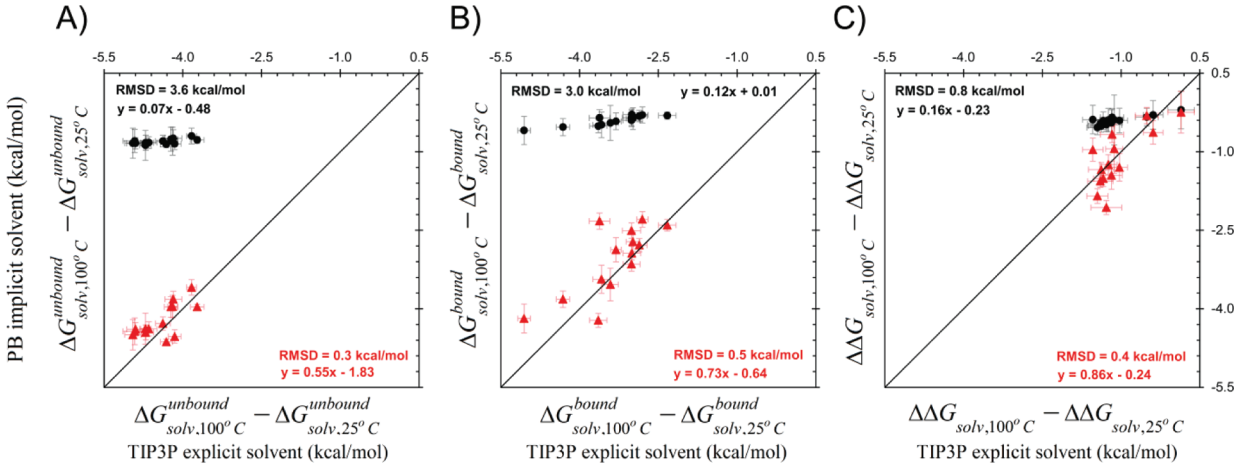


**Figure 3.** Comparison of the PB implicit solvent model and the TIP3P explicit solvent model for computing the solvation thermodynamics of salt bridges at 100 °C relative to 25 °C (in reference to their hydrophobic isosteres) in the absence of the protein environment: (A) solvation free energies in the unbound state $\Delta\Delta G_{solv}^{unbound}$, (B) solvation free energies in the bound state $\Delta\Delta G_{solv}^{bound}$, and (C) desolvation penalties upon association $\Delta\Delta G_{solv} = \Delta G_{solv}^{unbound} - \Delta G_{solv}^{bound}$. Implicit solvent simulations were performed with and without a radius scaling factor (RSF) (red triangles and black circles, respectively). The diagonal lines represent perfect agreement; the rmsds and equations for the linear regression in the bottom right and upper left corners of the plots correspond to implicit solvent calculations with and without the inclusion of an RSF, respectively. Error bars were calculated as described in Methods.

involving the same set of salt bridges at 25 °C.[14] We summarize the key details of the calculations below.

**Implicit Solvent Calculations.** Implicit solvent calculations were performed using finite difference methods, as implemented in the DelPhi 4.0 software package,[32] to solve the linearized form of the PB equation; this equation reduces to the Poisson equation in the absence of salt, as in our calculations. To represent the boundary between the low-dielectric protein region and high-dielectric solvent region, the standard molecular surface was used.[33] Consistent with keeping the proteins rigid, a dielectric constant of 1 was used for the protein region; to model solvation at 100 °C, the solvent dielectric constant was set to the experimental value for water at 100 °C (55.55, compared to 78.4 at 25 °C).[34] In addition, we tested the effects of scaling the atomic radii using a temperature-dependent radius scaling factor (RSF) that has been empirically derived for 100 °C: 1.012 for the $NH_3^+$ and guanidinium groups, 1.036 for carboxyl groups, and 1.046 for all other groups.[13] Consistent with the explicit solvent calculations, periodic boundary conditions were employed, implicitly including long-range electrostatic interactions with all periodic images. Electrostatic contributions to solvation free energies were determined by first directly calculating the induced polarization charges and then calculating the interaction between the protein charges and the reaction field due to the polarization charges.[35] The resulting electrostatic contributions are averages of 14 calculations involving systematic molecular translations on the grid, with uncertainties represented by the standard deviation. The electrostatic contribution to the solvation free energy of each salt bridge relative to its hydrophobic isostere in the unbound or bound state yields the solvation free energies $\Delta G_{solv}^{unbound}$ or $\Delta G_{solv}^{bound}$, respectively. The desolvation penalty of each salt bridge relative to its hydrophobic isostere was then calculated using $\Delta\Delta G_{solv} = \Delta G_{solv}^{unbound} - \Delta G_{solv}^{bound}$. Nonpolar contributions to the solvation free energies were not calculated since these contributions are identical for the wild-type salt bridge and its hydrophobic isostere, canceling out in the evaluation of $\Delta G_{solv}^{unbound}$ and $\Delta G_{solv}^{bound}$.

**Explicit Solvent Calculations.** Explicit solvent calculations were performed using the thermodynamic integration approach with MD simulations in explicit solvent, as implemented in the GROMACS 4.0.4 software package.[36] In particular, we first calculated differences in the overall free energies of each salt bridge relative to its hydrophobic isostere in its unbound and bound states. To obtain differences in solely the solvation free energies, all nonbonded protein−protein interactions were subtracted from differences in the overall free energies. The desolvation penalty of each salt bridge upon protein binding relative to its hydrophobic isostere was then calculated as the difference of the unbound and bound solvation energies. Separate MD simulations of the proteins (unbound and bound states) were performed in the NVT ensemble at each of eight $\lambda$ values, linearly reducing the partial charges of the side chains of the salt bridge from $\lambda = 0$ (wild-type) to $\lambda = 1$ (hydrophobic isostere). Results were considered converged if the uncertainty of each $\lambda$ simulation was small (<5%) and if the plot of $\langle \partial H(\lambda)/\partial\lambda \rangle_\lambda$ vs $\lambda$ was linear ($R^2 > 0.997$). Uncertainties in the free energies are derived from sampling errors in $\langle \partial H(\lambda)/\partial\lambda \rangle_\lambda$; errors at each $\lambda$ value were estimated using block averaging,[37] as implemented in the g_analyze utility of GROMACS.[36]

Each $\lambda$ simulation was performed for 1 ns at 100 °C in the NVT ensemble (constant number of atoms, volume, and temperature) using the Langevin thermostat (frictional coefficient of 1 $ps^{-1}$). Constant volume was enforced by solvating the unbound and bound states of each protein−protein complex in cubic boxes of explicit water (TIP3P,[26] TIP4P,[26] or SPC/E[27]) with identical volumes that allowed for a minimum solute-wall distance of 12 Å. To ensure a constant number of atoms in the unbound and bound states, extra water molecules were removed from the bound state, which contained more water molecules than the unbound state in all cases. This removal was done before energy minimization of the entire system and subsequent equilibration of the solvent; both minimization and equilibration were performed prior to the production phase of each $\lambda$ simulation. Equilibration of the solvent was performed in two stages: (1) 10 ps at constant temperature (100 °C) and volume and (2) 100 ps at constant


dx.doi.org/10.1021/jp210172b | J. Phys. Chem. B 2012, 116, 2561−2567

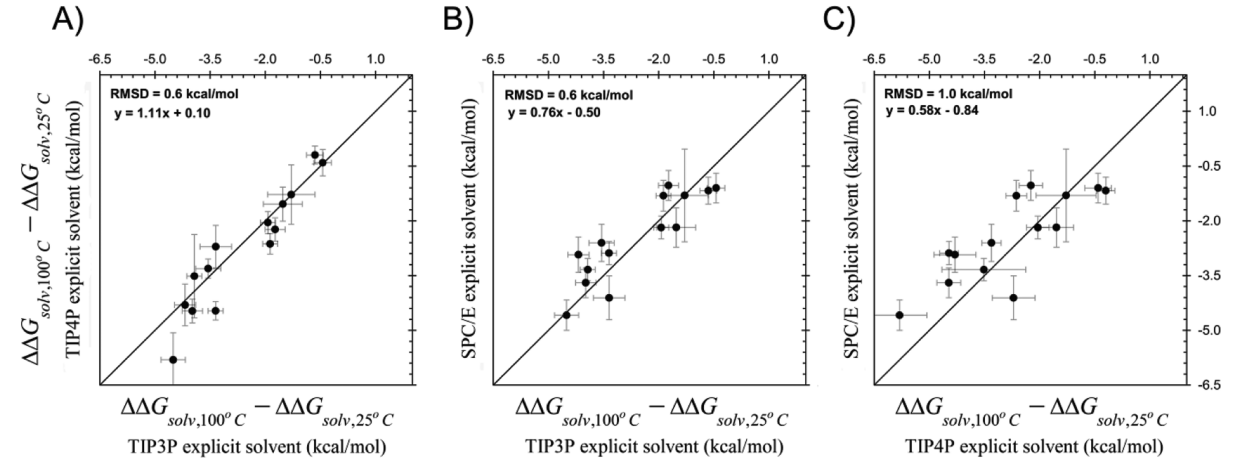


**Figure 4.** Comparison of explicit solvent models for computing the desolvation penalty of salt bridges upon protein−protein binding at 100 °C relative to 25 °C (in reference to their hydrophobic isosteres): (A) TIP4P vs TIP3P, (B) SPC/E vs TIP3P and (C) SPC/E vs TIP4P. Diagonal lines represent perfect agreement; the rmsds and equations for the linear regression are displayed in the upper left corners of the plots.

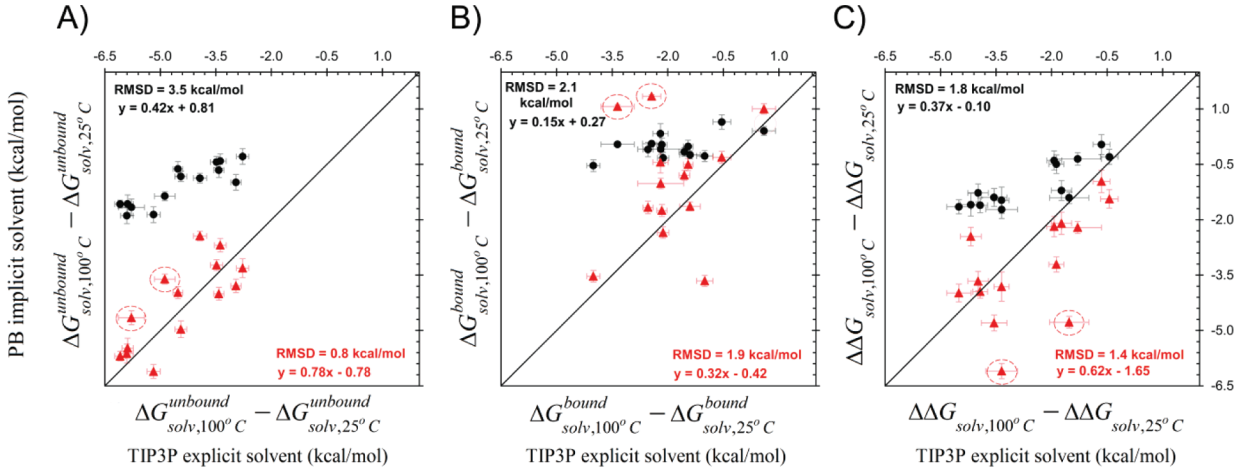


**Figure 5.** Comparison of implicit and explicit solvent models for computing the solvation thermodynamics of salt bridges at 100 °C relative to 25 °C (in reference to their hydrophobic isosteres) in the context of the proteins: (A) solvation free energies in the unbound state $\Delta\Delta G_{solv}^{unbound}$, (B) solvation free energies in the bound state $\Delta\Delta G_{solv}^{bound}$, and (C) desolvation penalties upon association $\Delta\Delta G_{solv} = \Delta G_{solv}^{unbound} - \Delta G_{solv}^{bound}$. Implicit solvent simulations were performed with and without a radius scaling factor (RSF) (red triangles and black circles, respectively). The diagonal lines represent perfect agreement; the rmsds and equations for the linear regression trend line in the bottom right and upper left corners of the plots correspond to implicit solvent calculations with and without the inclusion of an RSF, respectively. Error bars were calculated as described in Methods. Outliers discussed in the text are highlighted with dashed red circles.

temperature (100 °C) and pressure (1 atm). Throughout all stages of the simulations, the proteins were kept rigid using the GROMACS frozen option, which sets the velocities of all protein atoms to 0. Real space electrostatic interactions were truncated at 10 Å, while the long-range components of these interactions were calculated using the PME method[30] with periodic boundary conditions. Van der Waals interactions were switched off smoothly between 8 and 9 Å. A 2 fs time step was used for all simulations.

## RESULTS AND DISCUSSION

As discussed above, we focused our comparison of implicit and explicit solvent models on computing desolvation penalties of salt bridges at 100 °C relative to 25 °C. We first performed calculations on the 14 salt bridges in the absence of the protein environment, that is, with the same geometries, but in solution and with the residues capped with acetyl and *N*-methyl groups at the N- and C-termini, respectively. We then performed calculations on the same set of salt bridges in the context of the proteins. In both the absence and presence of the protein environment, we examined the effect of including a temperature-dependent radius scaling factor (RSF) on the implicit solvent results.

**Salt Bridges in the Absence of the Protein Environment.** In our calculations involving the salt bridges in solution, only the TIP3P water model was used for the explicit solvent calculations. Figure 3C shows the correlation between the desolvation penalties of the salt bridges at 100 °C relative to 25 °C (in reference to their hydrophobic isosteres) for the PB implicit calculations vs TIP3P explicit solvent calculations. As shown by previous studies,[8,28] the solvation free energies of the salt bridges become less favorable at high temperature, with the unbound state more adversely affected than the bound state, thereby reducing the magnitude of desolvation penalties incurred upon salt bridge formation. The resulting changes in the solvation free energies (in the unbound and bound states) as well as the desolvation penalties of the salt bridges are therefore expected to be negative in sign, as is the case in our


dx.doi.org/10.1021/jp210172b | J. Phys. Chem. B 2012, 116, 2561−2567

results (see Table S1, Supporting Information). This reduction in desolvation penalties is underestimated by the implicit solvent calculations when the atomic radii are not scaled with temperature. Upon scaling the atomic radii, the root-mean-square deviation (rmsd) is reduced from 0.8 to 0.4 kcal/mol, and the slope of the linear regression line increases from 0.16 to 0.86. The agreement of the implicit and explicit solvent results improves even more dramatically for the solvation free energies of the salt bridges in their unbound and bound states at 100 °C relative to 25 °C (Figure 3A, B, respectively; see also Tables S1 and S2, Supporting Information). These improvements, which are consistent with those reported for acetate and methyl ammonium associations, are encouraging given that the RSF was derived to reproduce the solvation free energies of amino acids from experiments rather than explicit solvent simulations.[13]

**Salt Bridges in the Context of the Proteins.** In our calculations involving the salt bridges in their protein environments, all three water models, TIP3P, TIP4P, and SPC/E, were tested for the explicit solvent calculations. The desolvation penalties of the salt bridges at 100 °C relative to 25 °C are similar for all of these explicit solvent models, with rmsds of 0.6, 0.6, and 1.0 kcal/mol for TIP4P versus TIP3P (Figure 4A), SPC/E versus TIP3P (Figure 4B), and SPC/E versus TIP4P (Figure 4C), respectively. Figure 5C shows the correlation between the desolvation penalties for the PB implicit calculations vs TIP3P explicit solvent calculations. As determined earlier for the corresponding salt bridges in the absence of their protein environments, these results reveal that the desolvation costs are reduced at high temperature (i.e., 100 °C) relative to room temperature. In contrast, however, inclusion of an RSF in the implicit solvent calculations only slightly improves the agreement between results for implicit and explicit solvent, regardless of the explicit water model (TIP3P, TIP4P, or SPC/E). For example, the rmsd is lowered from 1.8 to 1.4 kcal/mol and the slope of the trend line is increased from 0.37 to 0.62 for the TIP3P explicit water model (Figure 5C).

To determine the source of this improvement (and why it is small), we examined the correlations between implicit and explicit solvent calculations in terms of the solvation free energies of the salt bridges at 100 °C relative to 25 °C in their unbound and bound states (Tables S3–S6, Supporting Information). Inclusion of an RSF significantly reduces the implicit–explicit differences in the solvation free energies in the unbound states (Figure 5A), lowering the rmsd from 3.5 to 0.8 kcal/mol and increasing the slope from 0.42 to 0.78. At first glance, inclusion of the RSF appears to have little effect on the solvation free energies in the bound states (Figure 5B), with the rmsd remaining essentially the same (2.1 reduced to 1.9 kcal/mol), while the slope increases from 0.15 to 0.32. However, the apparent absence of improvement is largely due to two outliers with negative values from the explicit solvent calculations but unexpected positive values from the implicit solvent calculations. Once these outliers are removed, the rmsd improves from 1.9 to 1.1 kcal/mol, and the slope increases from 0.32 to 0.74. For the differences in desolvation penalties, the rmsd improves from 1.4 to 0.9 kcal/mol (the slope of ~0.6 remains essentially unchanged). These differences are comparable to those between different explicit solvent models (i.e., rmsd of 1.0 kcal/mol and slope of 0.58 for SPC/E vs TIP4P), which is remarkable given the dramatic differences between implicit and explicit solvent models.

**Further Examination of Outliers.** The two outliers in the bound state of the proteins (Figure 5B) correspond to the R83-D39 and R87-D39 salt bridges across the binding interface of the barnase–barstar complex (Figure 1). These salt bridges are the only ones among our set of 14 that are (a) completely buried in the bound state according to the implicit solvent model and (b) involved in a network where at least one of the charged partners (i.e., D39) forms another salt bridge[3,38] (Table S7, Supporting Information). We therefore wondered if this unique combination of features might be responsible for the large implicit–explicit discrepancies associated with these salt bridges, causing the implicit solvent results to be too unfavorable and/or the explicit solvent results to be too favorable.

We first compared the degree to which these salt bridges are buried in both the implicit and explicit solvent calculations. While these salt bridges are completely buried within the context of the implicit solvent model, they are partially solvated by three crystallographic water molecules[39] that remain relatively fixed in the surrounding protein cavity at the barnase–barstar interface throughout the explicit solvent simulations (Figure 6); two of these water molecules form

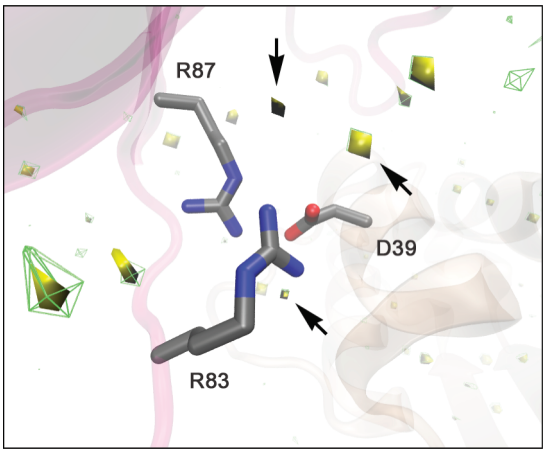


**Figure 6.** Most frequently visited positions (≥ 30% of the time) of water molecules in the vicinity of the R83-D39 and R87-D39 salt bridges during explicit solvent simulations of the wild-type barnase–barstar complex (no hydrophobic isosteres) at 100 and 25 °C (yellow solid and green mesh regions, respectively). The arrows indicate regions in the protein cavity surrounding the R83-D39 and R87-D39 salt bridges that are occupied by water molecules that are within 5 Å of the salt bridges. These regions correspond to the locations of three crystallographic water molecules, two of which form hydrogen bonds with the barstar Asp39 residue. To map out these positions, the simulation box was first divided into ~1 Å$^3$ cubes, and then, the number of oxygen atoms of the water molecules were counted in each cube using snapshot configurations that were collected every ps from a 1 ns simulation of the barnase–barstar complex (total of 1000 configurations).

hydrogen bonds with the barstar Asp39 residue. To determine the effect of this partial solvation, we first removed these confined water molecules and then repeated the explicit solvent calculations at both 100 and 25 °C. The resulting solvation free energies of the salt bridges in their bound states at 100 °C relative to 25 °C ($\Delta G^{bound}_{solv,100°C} - \Delta G^{bound}_{solv,25°C}$) became less favorable and thereby closer in agreement with the implicit solvent results, increasing from −2.4 ± 0.2 to −1.7 ± 0.4 kcal/mol for the R83-D39 salt bridge and from −3.4 ± 0.4 to −1.8 ±


dx.doi.org/10.1021/jp210172b | J. Phys. Chem. B 2012, 116, 2561–2567

0.3 kcal/mol for the R87-D39 salt bridge (uncertainties were computed as described in Methods). It appears therefore that the difference in solvent exposure of these salt bridges in the implicit vs explicit solvent calculations is a source of the large implicit−explicit discrepancies in the effects of increasing temperature on the solvation free energy of the bound state. This difference arises because the implicit solvent model is not sufficiently detailed to capture the full complexity of the molecular surface at the protein−protein interface.

Next, we examined the contribution of the R83-D39-R87 salt bridge network to the implicit−explicit solvent discrepancies associated with the R83-D39 and R87-D39 salt bridges. In particular, for each of these two salt bridges, we first disrupted the network by mutating the other member of the network to its hydrophobic isostere (i.e., for the R83-D39 salt bridge, R87 is mutated; for the R87-D39 salt bridge, R83 is mutated) and then performed another set of both implicit and explicit solvent calculations for that salt bridge at 100 and 25 °C to evaluate the solvation free energies of the salt bridges in their bound states at 100 °C relative to 25 °C. While the explicit solvent results became even more negative (decreasing from −2.4 ± 0.2 to −6.2 ± 0.8 kcal/mol for the R83-D39 salt bridge and from −3.4 ± 0.4 to −4.4 ± 0.3 kcal/mol for the R87-D39 salt bridge), the implicit solvent results decreased from positive values to just zero. These results indicate that the implicit treatment of solvent somehow falls short of explicit solvent models in capturing the effects of high temperature on the solvation free energies of buried, networked salt bridges in their bound states. This limitation, in combination with the difference in solvent exposure between the implicit and explicit solvent calculations, appears to be at least partially responsible for the large implicit−explicit discrepancies associated with these salt bridges.

## CONCLUSIONS

In conclusion, we performed a direct comparison of implicit and explicit solvent models in computing the desolvation penalties of salt bridges across a number of protein−protein interfaces at 100 °C relative to 25 °C. With the exception of two outliers, the implicit and explicit solvent results are of similar magnitudes and significantly reduced at 100 °C relative to 25 °C. As proposed previously based on solely implicit solvent calculations, the reduction in desolvation penalties at high temperature is a potential explanation for salt bridges playing crucial roles in promoting hyperthermostability in proteins despite making little favorable contribution to protein stability at room temperature.[8] Our study demonstrates that this proposal is also supported by more detailed explicit solvent calculations, based on the general agreement between our implicit and explicit solvent results. This agreement demonstrates that implicit solvent models can be comparable to explicit solvent models in their ability to quantitatively account for the effects of increasing the temperature from 25 to 100 °C on the solvation thermodynamics of proteins. Nonetheless, significant discrepancies exist for particular salt bridges, i.e., the two pairs in which the salt bridges are part of a salt bridge network that is completely buried in the implicit solvent model but partially exposed to solvent in the explicit solvent simulations. For these salt bridges, the implicit solvent model does not appear to be sufficiently detailed to capture the effects of increasing temperature on the solvation thermodynamics, even after appropriate adjustment of its temperature-dependent parameters. Given the potential importance of salt bridge networks in proteins[38] and protein−protein complexes,[40] these challenging cases should be considered in the development of fast solvation approaches.

## ASSOCIATED CONTENT

### Supporting Information

Computed desolvation penalties and solvation free energies and percent burial of salt bridges. This material is available free of charge via the Internet at http://pubs.acs.org.

## AUTHOR INFORMATION

### Corresponding Author

*E-mail: ltchong@pitt.edu.

### Notes

The authors declare no competing financial interest.

## ACKNOWLEDGMENTS

We thank Matt Zwier for constructive comments on this manuscript. This work was supported by the NSF (CAREER MCB-0845216 and XSEDE MCB100109) and an Arts & Sciences Fellowship from the University of Pittsburgh to R.S. Computational resources were also provided by the Center for Simulation and Modeling at the University of Pittsburgh.

## REFERENCES

(1) Novotny, J.; Sharp, K. A. *Prog. Biophys. Mol. Biol.* **1992**, *58*, 203.
(2) Hendsch, Z. S.; Tidor, B. *Protein Sci.* **1999**, *8*, 1381.
(3) Sheinerman, F. B.; Honig, B. *J. Mol. Biol.* **2002**, *318*, 161.
(4) Sterner, R.; Liebl, W. *Crit. Rev. Biochem. Mol. Biol.* **2001**, *36*, 39.
(5) Vieille, C.; Zeikus, G. J. *Microbiol. Mol. Biol. Rev.* **2001**, *65*, 1.
(6) Kumar, S.; Nussinov, R. *Cell. Mol. Life Sci.* **2001**, *58*, 1216.
(7) Karshikoff, A.; Ladenstein, R. *Trends Biochem. Sci.* **2001**, *26*, 550.
(8) Elcock, A. H. *J. Mol. Biol.* **1998**, *284*, 489.
(9) Sitkoff, D.; Sharp, K. A.; Honig, B. *J. Phys. Chem.* **1994**, *98*, 1978.
(10) Nina, M.; Beglov, D.; Roux, B. *J. Phys. Chem.* **1997**, *101*, 5239.
(11) Swanson, J. M. J.; Adcock, S. A.; McCammon, J. A. *J. Chem. Theory Comput.* **2005**, *1*, 484.
(12) Zhu, S.; Elcock, A. H. *J. Chem. Theory Comput.* **2010**, *6*, 1293.
(13) Elcock, A. H.; McCammon, J. A. *J. Phys. Chem. B* **1997**, *101*, 9624.
(14) Salari, R.; Chong, L. T. *J. Phys. Chem. Lett.* **2010**, *1*, 2844.
(15) Yu, Z. Y.; Jacobson, M. P.; Josovitz, J.; Rapp, C. S.; Friesner, R. A. *J. Phys. Chem. B* **2004**, *108*, 6643.
(16) Wagoner, J. A.; Baker, N. A. *Proc. Natl. Acad. Sci. U.S.A.* **2006**, *103*, 8331.
(17) Zhang, L. Y.; Gallicchio, E.; Friesner, R. A.; Levy, R. M. *J. Comput. Chem.* **2001**, *22*, 591.
(18) Tan, C.; Yang, L.; Luo, R. *J. Phys. Chem. B* **2006**, *110*, 18680.
(19) Thomas, A. S.; Elcock, A. H. *J. Am. Chem. Soc.* **2006**, *128*, 7796.
(20) Shang, Y.; Nguyen, H.; Wickstrom, L.; Okur, A.; Simmerling, C. *J. Mol. Graphics Modell.* **2011**, *29*, 676.
(21) Wang, J.; Tan, C.; Chanco, E.; Luo, R. *Phys. Chem. Chem. Phys.* **2010**, *12*, 1194.
(22) Green, D. F.; Tidor, B. *Proteins* **2005**, *60*, 644.
(23) Altman, M. D.; Nalivaika, E. A.; Prabu-Jeyabalan, M.; Schiffer, C. A.; Tidor, B. *Proteins* **2008**, *70*, 678.
(24) Kajander, T.; Sachs, J. N.; Goldman, A.; Regan, L. *J. Biol. Chem.* **2009**, *284*, 25364.
(25) Carrascal, N.; Green, D. F. *J. Phys. Chem. B* **2010**, *114*, 5096.
(26) Jorgensen, W.; Chandrasekhar, J.; Madura, J.; Impey, R.; Klein, M. *J. Chem. Phys.* **1983**, *79*, 926.
(27) Berendsen, H. J. C.; Grigera, J. R.; Straatsma, T. P. *J. Phys. Chem.* **1987**, *91*, 6269.
(28) Thomas, A. S.; Elcock, A. H. *J. Am. Chem. Soc.* **2004**, *126*, 2208.
(29) Kaminski, G. A.; Friesner, R. A.; Tirado-Rives, J.; Jorgensen, W. L. *J. Phys. Chem. B* **2001**, *105*, 6474.

(30) Essmann, U.; Perera, L.; Berkowitz, M. L.; Darden, T.; Lee, H.; Pedersen, L. G. *J. Chem. Phys.* **1995**, *103*, 8577.
(31) Bogusz, S.; Cheatham, T. E. III; Brooks, B. R. *J. Chem. Phys.* **1998**, *108*, 3017.
(32) Honig, B.; Nicholls, A. *Science* **1995**, *268*, 1144.
(33) Rocchia, W.; Sridharan, S.; Nicholls, A.; Alexov, E.; Chiabrera, A.; Honig, B. *J. Comput. Chem.* **2002**, *23*, 128.
(34) Archer, D. G.; Wang, P. *J. Phys. Chem. Ref. Data* **1990**, *19*, 371.
(35) Dong, F.; Zhou, H.-X. *Proteins* **2006**, *65*, 87.
(36) Hess, B.; Kutzner, C.; van der Spoel, D.; Lindahl, E. *J. Chem. Theory Comput.* **2008**, *4*, 435.
(37) Bishop, M.; Frinks, S. *J. Chem. Phys.* **1987**, *87*, 3675.
(38) Kumar, S.; Nussinov, R. *J. Mol. Biol.* **1999**, *293*, 1241.
(39) Buckle, A. M.; Schreiber, G.; Fersht, A. R. *Biochemistry* **1994**, *33*, 8878.
(40) Sheinerman, F. B.; Norel, R.; Honig, B. *Curr. Opin. Struct. Biol.* **2000**, *10*, 153.